Journal of Nuclear Materials 141–143 (1986) 536–539
North-Holland, Amsterdam

COMPREHENSIVE MODELING OF CREEP FRACTURE BY GRAIN BOUNDARY CAVITATION IN IRRADIATED STRUCTURAL ALLOYS*

J.N. AL-HAJJI[1] and Nasr M. GHONIEM[2]

[1]*Mechanical Engineering Department, Kuwait University, P.O. Box 5969, Kuwait*
[2]*Mechanical, Aerospace and Nuclear Engineering Department, University of California, Los Angeles, CA 90024, USA*

The present model describes high-temperature helium embrittlement as a sequence of four steps. First, helium clustering in the matrix is described by the conventional rate theory. This is coupled to rate equations for the transport of single helium atoms to grain boundaries in the second phase. The third step is concerned with the influence of helium and stress on the nucleation of cavities at GBs, with particular emphasis on the role that precipitates and triple-point junctions play in the nucleation process. Finally, various growth modes of grain boundary cavities which lead to fracture by the inter-linkage of equally spaced GB cavities are investigated.

In this paper, a description of this comprehensive model is given, with emphasis on the growth and inter-linkage of grain boundary cavities under the effects of irradiation and applied stress. A comparison between the model predictions and recent experimental creep rupture data is given. The model proposes a new explanation of the creep rupture behavior of martensitic steels as opposed to austenitic steels. Vacancy source limitation at GBs resulting from dislocation interactions is identified as the primary reason for the retarded growth of GB cavities in martensitics.

1. Introduction

Fracture of alloys at high temperature is now widely recognized to result from the influence of the applied stress on the nucleation and growth of grain boundary (GB) cavities. Several investigators have proposed theoretical models to describe the mechanistic physical process underlying this important phenomenon. For convenience, theories in this area have tended to address either the nucleation phase of cavities (e.g., refs. [1–4]), or the growth mechanisms controlling the rapid expansion of GB cavities under the influence of an applied stress at high temperature (e.g., refs. [5–8]). During irradiation in a neutron environment, other physical processes must be considered. Energetic neutrons displace lattice atoms creating Frenkel pairs, and also produce substantial amounts of hydrogen and helium. Point-defect diffusion enhances non-equilibrium rate processes governing microstructure evolution; hence, the nucleation and growth phases of GB cavities. On the other hand, helium, which has low solubility in most metals, tends to segregate within the matrix before reaching grain boundaries.

A host of interesting questions arise when one attempts to understand the importance of variables controlling the grain boundary fracture process. Experiments have shown that temperature, stress, displacement damage, helium production, as well as material variables influence grain boundary fracture. The present model is an effort to unravel the actions of some of these mechanisms and to explain, by comparison with experimental data, the differences in the behavior of austenitic and martensitic alloys. First we summarize our work in two areas: helium transport to GBs and GB cavity nucleation under irradiation. Next, delineation of GB cavity growth and fracture is presented as a part of an integrated model of high-temperature fracture under irradiation. Finally, results and conclusions are given in section 4.

2. Helium transport and GB cavity nucleation

A rate theory formalism has been recently developed by Ghoniem, Al-Hajji and Kalleta [9] to analyze the problem of helium clustering in the matrix and its transport to GBs. Furthermore, the problem of GB cavity nucleation under the combined influence of helium generation and an applied stress has been presented in another publication [10]. Fundamental rate equations are developed and numerically solved for a number of helium-vacancy clusters which describe helium clustering and transport to grain boundaries. Conservation equations are solved for single vacancies, single interstitials, interstitial helium atoms, substitutional helium, relevant helium-vacancy clusters which lead to the direct (spontaneous) nucleation of helium-filled cavities, the concentration to matrix cavities, the average number of helium atoms in a cavity, the average radius of various matrix cavities, and finally the rate of transport of helium atoms to the grain boundary.

The work reveals interesting facets of helium behavior in the presence of Frenkel pairs resulting from displacement damage. If the helium production rate is significant, as is expected in fusion reactor first-wall materials, vacancies are immobilized in the matrix resulting in a slow mode of growth for matrix cavities. This effect, coupled with a high rate of gas re-solution from cavities, is shown to result in continuous (dynamic) nucleation throughout irradiation.

* This work was supported by the US Department of Energy, Office of Fusion Energy, Grant #DE-FG03-84ER52110, with UCLA.

The matrix cavity structure can be characterized by a uniform population of small cavities, with the exception of those associated with precipitates. During early irradiation, helium gas is trapped in small vacancy clusters. The nucleation and subsequent growth of matrix cavities reduces the chances of helium migrating to the grain boundary because newly introduced helium can now be absorbed at matrix cavities and precipitates. It is found that the time-dependent flux of helium arriving at grain boundaries is controlled by the dynamic matrix clustering processes. To reduce this harmful amount of helium, trapping in the matrix must be further enhanced through the introduction of a uniform concentration of precipitates in the matrix, as is experimentally observed [11]. The only real limitation of this method of alloy tailoring is the possible concomitant reduction in ductility.

The nucleation of GB cavities is treated as a consequence of a combination of applied stress and helium escaping from the matrix, as determined by the previous step [10]. A modification to classical nucleation theory to account for site occupancy at triple-point junctions and GB precipitates leads to the following equation [10]:

$$\dot{C} = (C_{\max} - C)\left[\left(\frac{\pi}{12F_v\gamma_s^3 kT}\right)^{1/2}\sigma_L^2 D_b\delta\exp\left(-\frac{\Delta G_c}{kT}\right)\right], \quad (1)$$

where $C_{\max}$ is the maximum number of available nucleation sites per unit area of GBs, F_v is the volumetric shape factor, δ_s is the cavity surface energy, k is Boltzmann's constant, T is the temperature, δ is the boundary thickness, σ_L is the local stress, D_b is the grain boundary diffusivity, and and ΔG_c is the change in free energy resulting from the introduction of cavities on a stressed boundary.

Local stress loading and unloading is phenomenologically modeled at triple-point junctions and GB-precipitate interfaces. The resulting time-dependent stress is introduced in eq. (1), which is subsequently numerically integrated. The influence of helium on GB cavity nucleation is studied via rate theory. Appropriate hierarchial equations are simultaneously solved for the helium-induced nucleation of GB cavities. Reasonable correlation with experimental data [12] has been achieved for an effective helium migration energy close to the self-diffusion energy.

Grain boundary inclination to the principal direction of the applied stress is found to be an important parameter and it displays a great influence on the rate of cavity nucleation. It is assumed in this work that irregularities with inclinations on the order to 10 to 20° occur at normal boundaries. Depending on the inclination angle, available nucleation sites could be saturated during one stress loading and unloading pulse for large inclinations, or they may require a number of such repetitive pulses. This will depend on the stochastic nature of stress localization due to sliding.

Helium, on the other hand, is found to lead to rapid homogeneous nucleation of cavities on the GB; the quasi-steady-state density being reached at 1 to 10 appm helium. The work shows that, consistent with experiments, irradiation-generated GB bubble densities are generally orders of magnitude greater than those observed in creep experiments in the absence of irradiation. Small amounts of total injected helium ($\simeq 1$ appm He) may result in GB bubble densities as high as 10^{13} m^{-2}. During irradiation, it can be safely assumed that nucleation of GB cavities is rapidly achieved, and that the majority of cavity lifetime is spent in the growth regime.

3. Grain boundary cavity growth and fracture

Earlier growth models of GB cavities have assumed that the GB is essentially an inexhaustible source of vacancies that are readily available for cavities (e.g., refs. [4–7]). However, a recent review by Balluffi stresses the importance of the relationship between the boundary structure and the availability of vacancies [13]. Bollmann's [14] formal theory of crystalline interfaces demonstrates that it is always possible for a lattice dislocation to enter the boundary upon impingement. Fig. 1 shows a schematic representation of a model for

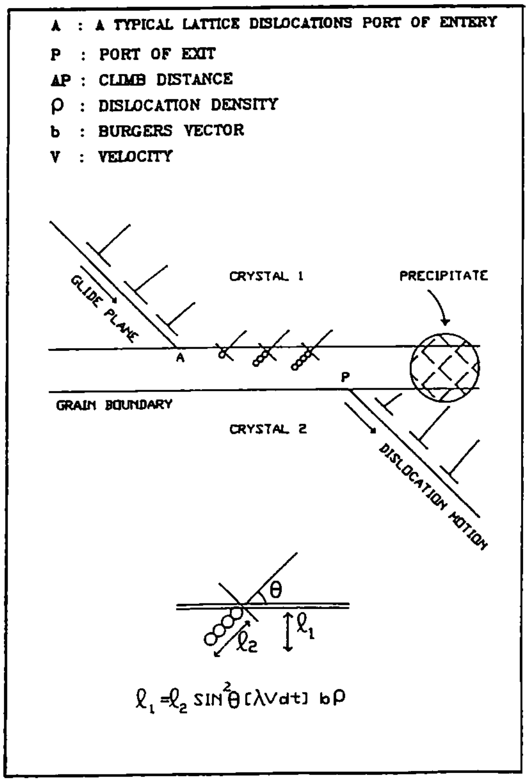

Fig. 1. A schematic illustration of lattice dislocation interactions with grain boundaries.

the vacancy-source control by dislocations at GBs; the model is similar to that of Beere [15]. The model illustrated in fig. 1 is a general representation which includes the possibilities that lattice dislocations may enter or leave the boundary. By climbing in both the lattice and the boundary, dislocations can dictate the rate of vacancy creation within the boundary. Adopting Beere's approach, various growth mechanisms can be viewed as sharing mixed sequential/independent relationships. The overall volumetric cavity growth rate $\dot{V}$ is given by:

$$\dot{V} = \dot{V}_{DC} + \frac{\dot{V}_{BD}\dot{V}_{SC}}{\dot{V}_{BD} + \dot{V}_{SC}}, \tag{2}$$

where $\dot{V}_{DC}$ is the growth rate due to dislocation creep, $\dot{V}_{BD}$ is the GB diffusion growth rate, and $\dot{V}_{SC}$ is the vacancy-source-controlled growth rate.

Following Speight and Harris [16], the cavity growth rate due to boundary diffusion is calculated. The cavity radial growth rate, dR/dt, is given by

$$\frac{dR}{dt} = \frac{4\pi}{3}\frac{\sin^3\phi}{F_v}\frac{\delta D_{gb}\Omega}{L^2kT}\left(p + \sigma - \frac{2\gamma_s \sin\phi}{R}\right) \times \left[\frac{(L/R)^2 - 1}{2\ell n(L/R) - 1 + (R/L)^2}\right], \tag{3}$$

where ϕ is the contact angle of a lenticular cavity, L is the inter-cavity half spacing, p is the internal helium gas pressure, and σ is the normal component of the stress. The radial velocity is quite fast, and is reduced by control of the vacancy supply. The volumetric growth rate due to vacancy source control is given by

$$\dot{V}_{SC} = \frac{\pi^2}{4} L^2\lambda\dot{\varepsilon}\left(\frac{1 - 2\gamma_s \sin\phi/R\sigma + p/\sigma}{1 - R^2/L^2}\right)^n, \tag{4}$$

where λ is the GB dislocation climb distance before the re-emission, $\dot{\varepsilon}$ is the matrix dislocation creep rate, and n the creep exponent.

Cavities can also grow by plastic deformation, as shown by Hancock [7]. The volumetric growth rate is given by

$$\dot{V}_{DC} = \frac{3R^3F_v}{\sin^3\phi}\dot{\varepsilon}\left(\frac{1 - 2\gamma_s \sin\phi/R\sigma + p/\sigma}{1 - R^2/L^2}\right)^n. \tag{5}$$

Details of eqs. (1)–(4) are given in ref. [17].

Numerical calculations were performed for eq. (2), using eqs. (3)–(5) and assuming that the cavity shape is lenticular. It is found that a growth instability takes place when the average cavity radius is about 60% of the average inter-cavity spacing. Experimental evidence [18] indicates that GB cavity growth rates are much smaller in ferritic/martensitic alloys as compared with austinitics. Significant ductile deformation occurs in martensitics before fracture, as opposed to a much more limited ductility in austenitics. Wassilew [18] argues that twinning is the major reason for this observed discrepancy. Twin planes are assumed to supply the necessary vacancy source in austenitics, while twinning does not take place in martensitics. However, this interpretation does not explain why cavities at the intersection of the few twin planes and the GBs do not grow much faster than the remainder of the population.

In this work, we consider the process of matrix dislocation entry/exit in the GB. Slip is the prinicpal means by which plastic deformation occurs in crystalline solids. While an austenitic steel (FCC) has 12 slip systems, a martensitic alloy (BCC) would have 48. Cross-slip in BCC systems allows for much easier dislocation motion. Observed creep rates and dislocation recovery processes are higher in martensitic alloys than in austenitic, which is commensurate with faster dislocation recovery. Since the average dislocation residence time is determined by the average distance between entry and exit planes at the GB, it is expected that this time is shorter in a martensitic alloy. This will naturally place a vacancy source limitation on the growth rate of GB cavities in martensitics. We assume here that the average GB dislocation climb distance in austenitic alloys is the GB interprecipitate spacing. Because of the easier dislocation motion in martensitics, this distance is assumed to be on the order of the GB inter-bubble spacing.

4. Results and conclusions

The model described in this paper is a comprehensive on involving detailed computations and various levels of approximations. Helium embrittlement is a complex phenomenon, and comparisons with experiments should still be taken cautiously. Unlike earlier attempts to explain experiments on the basis of one mechanism (e.g., refs. [18,19]), this work attempts to treat the problem in a self-consistent way. Fig. 2 compares the calculated and experimentally measured

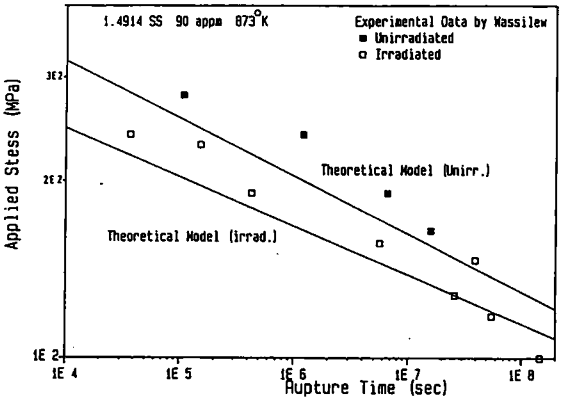

Fig. 2. A comparison of calculated and experimental time-to-rupture for the martensitic stainless steel DIN 1.4914 at 873 K. The neutron fluence is 1.05×10^{26} n/m^2, $E > 0.1$ MeV. (Data from ref. [20].)

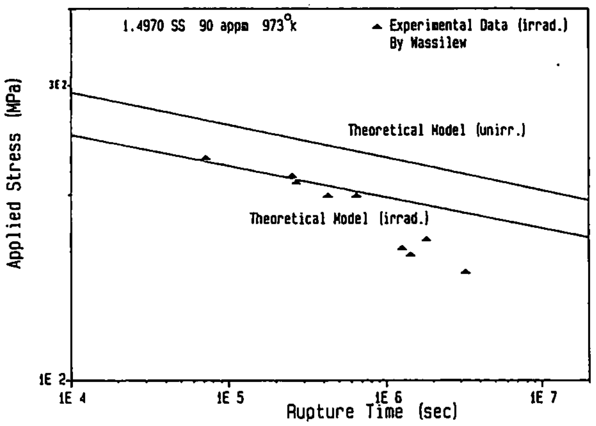

Fig. 3. A comparison of calculated and experimental time-to-rupture for the austenitic stainless steel DIN 1.4970 at 973 K. The neutron fluence is 3×10^{25} n/m^2, $E > 0.1$ MeV. (Data from ref. [20].)

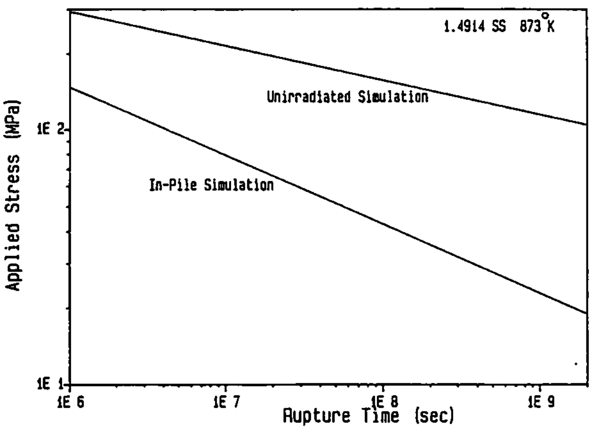

Fig. 4. A theoretical comparison of the stress dependence of the time-to-rupture of unirradiated and in-reactor tested martensitic stainless steel at 873 K. The neutron fluence is 1.05×10^{26} n/m^2, $E > 0.1$ MeV.

time-to-rupture for the German martensitic steel DIN 1.4914 at 600°C. The data are taken from ref. [20]. Here creep experiments were for post-irradiation conditions. The presence of helium does not drastically reduce the time-to-rupture. In fig. 3, the model suggests a higher sensitivity to helium for the corresponding austenitic alloy (DIN 1.4970). In fig. 4, we compare calculations of time-to-rupture data of the martensitic steel (DIN 1.4914), for both unirradiated and in-reactor behavior at 600°C. The main reason for this greater sensitivity is the acceleration of in-reactor creep in martensitics only, as was recently observed by Herschbach [21].

It is concluded here that even though GB cavities in martensitic alloys are sluggish in their growth behavior, raising possibilities for the mitigation of high-temperature embrittlement, the unfortunate creep acceleration because of irradiation may still limit the upper useful design temperature limit.

Support by the Kuwait University to one of us (JNA) is appreciated. Partial Support by the US Department of Energy, Office of Fusion Energy, Grant #DE-FG03-84ER52110, with UCLA is acknowledged.

References

[1] I. Servi and N.J. Grant, Trans. AIME 191 (1951) 909.
[2] J.E. Harris, Trans. Metall. Soc. AIME 233 (1965) 1509.
[3] R. Raj and M.F. Ashby, Acta Metall. 23 (1975) 653.
[4] A.S. Argon, I.W. Chen and C.W. Lau, in: Creep-Fatigue-Environment Interactions, Eds. R.M. Pelloux and N.S. Stoloff (AIME, New York, 1980) p. 46.
[5] R.W. Balluffi and L.L. Seigle, Acta Metall. 3 (1955) 170.
[6] D. Hull and D.E. Rimmer, Philos. Mag. 4 (1959) 673.
[7] J.W. Hancock, Met. Sci. J. 10 (1976) 319.
[8] W. Beere and M.V. Speight, Met. Sci. J. 12 (1978) 172.
[9] N.M. Ghoniem, J.N. Al-Hajji and D. Kaletta, J. Nucl. Mater. 135 (1985) 192.
[10] J.N. Al-Hajji and N.M. Ghoniem, Acta Metall., submitted.
[11] H. Schroeder, W. Kesternick and H. Ullmaier, Nucl. Engrg. Des./Fusion 2 (1984) 65.
[12] A.L. Lane and P.J. Goodhew, Philos. Mag. A48 (1983) 965.
[13] R.W. Balluffi, in: Interfacial Segregation, Eds. W.C. Johnson and J.M. Blakely (ASM, Metals Park, OH, 1979) p. 193.
[14] W. Bollman, Crystal Defects and Crystalline Interfaces (Springer Verlag, Berlin, New York, 1970).
[15] W. Beere, Res Mechanica 2 (1981) 189.
[16] M.V. Speight and J.E. Harris, Met. Sci. J. 1 (1967) 83.
[17] J.N. Al-Hajji, Theoretical modeling of the high temperature helium in structural alloys, UCLA Ph.D. thesis (1985); also UCLA report ENG-8533/PPG-894 (1985).
[18] C. Wassilew, in: Proc. Int. Conf. on Mechanical Behavior and Nucl. Applications of Stainless Steel at Elevated Temperatures, The Metals Society, Varese, Italy, 1981, p. 172.
[19] K.L. Kear and M.H. Wood, An analysis of grain boundary failure in austenitic stainless steel, AERE-Harwell Report, AERE-R 10907 (1983).
[20] C. Wassilew, W. Kunischaud and B. Ritter, Institute für Material- und Festkörperforschung II, Report KFK PSB-Ber. 2035 (K1.III), Karlsruhe, West Germany (1981).
[21] K. Herschbach, J. Nucl. Mater. 127 (1985) 239.